

***E2* excitation strength in ^{55}Ni : Coupling of the ^{56}Ni 2_1^+ collective core vibration to the $f_{7/2}$ odd neutron hole**

K. L. Yurkewicz,^{1,2} D. Bazin,¹ B. A. Brown,^{1,2} C. M. Campbell,^{1,2} J. A. Church,^{1,2,*} D.-C. Dinca,^{1,2} A. Gade,¹ T. Glasmacher,^{1,2} M. Honma,³ T. Mizusaki,⁴ W. F. Mueller,¹ H. Olliver,^{1,2} T. Otsuka,^{5,6} L. A. Riley,⁷ and J. R. Terry^{1,2}

¹National Superconducting Cyclotron Laboratory, Michigan State University, East Lansing, Michigan 48824, USA

²Department of Physics and Astronomy, Michigan State University, East Lansing, Michigan 48824, USA

³Center for Mathematical Sciences, University of Aizu, Tsuruga, Ikki-machi, Aizu-Wakamatsu, Fukushima 965-8580, Japan

⁴Institute of Natural Sciences, Senshu University, Higashimita, Tama, Kawasaki, Kanagawa 214-8580, Japan

⁵Department of Physics and Center for Nuclear Study, University of Tokyo, Hongo, Tokyo 113-0033, Japan

⁶RIKEN, Hirosawa, Wako-shi, Saitama 351-0198, Japan

⁷Department of Physics and Astronomy, Ursinus College, Collegeville, Pennsylvania 19426, USA

(Received 6 August 2004; published 27 December 2004)

The collectivity of the odd-mass nucleus ^{55}Ni was explored via intermediate-energy Coulomb excitation using a powerful combination of particle and γ -ray spectroscopy. A γ -ray at 2879(18) keV was observed and is interpreted to deexcite a member of the core-coupled quintuplet $2_1^+(^{56}\text{Ni}) \otimes \nu f_{7/2}^{-1}$ at the same energy. By similarity with the mirror nucleus ^{55}Co , transition probabilities were calculated assuming $J^\pi=9/2^-$ and $J^\pi=11/2^-$ for this state. Both assumptions lead to a transition strength higher than predicted by a large-scale shell-model calculation using the GXPF1 effective interaction and exceed the value predicted within a simple weak-coupling approach.

DOI: 10.1103/PhysRevC.70.064321

PACS number(s): 27.40.+z, 25.70.De, 23.20.Lv, 23.20.Js

Intermediate-energy Coulomb excitation [1] of the projectile is a sensitive probe to investigate quadrupole collectivity in exotic nuclei. In the past, this method has been extensively used to determine the absolute $B(E2 \uparrow) = B(E2; 0_1^+ \rightarrow 2_1^+)$ excitation strength in even-even nuclei beyond the valley of β stability [2–5]. In odd- A nuclei, core-coupled states are accessible to the method of Coulomb excitation. These states can qualitatively be described as originating from a particle or hole weakly coupled to the even-even core [6]. In ^{55}Ni , the coupling of the $\nu f_{7/2}^{-1}$ neutron hole to the 2_1^+ excited state of the ^{56}Ni core should give rise to a quintuplet of negative-parity states with spin values $3/2^-$, $5/2^-$, $7/2^-$, $9/2^-$, and $11/2^-$. The region of the nuclear chart around the self-conjugate, doubly-magic nucleus ^{56}Ni has attracted much attention in recent years. The measurement of a large $B(E2 \uparrow)$ value [7–9], indicating an unexpectedly high degree of collectivity, prompted questions about the magicity of $N=Z=28$ [10]. So for example is the $B(E2)$ strength in Weisskopf units for the excitation of the first 2^+ state in ^{56}Ni four times larger than the corresponding value in the doubly magic $N=Z=20$ nucleus ^{40}Ca [11].

No transition strengths have been measured for ^{55}Ni until now. Spin and parity of $7/2^-$ for the ^{55}Ni ground state was determined from the measured β -strength in the decay to ^{55}Co [12,13]. Particle spectroscopy of the nucleus has revealed 20 low-lying levels including one at 2888(7) keV, but could not assign spins and parities [14]. A more recent gamma-sphere experiment aiming to measure the high-spin structure of ^{55}Ni identified four γ rays from the deexcitation of ^{55}Ni , including one with an energy of 2882(2) keV which is

interpreted to establish an excited state at the same energy [15]. Spin and parity of $11/2^-$ for the 2882 keV excited state could tentatively be assigned from the γ -ray angular distribution. Symmetry of the observed 2882 keV level with the corresponding $11/2^-$ state of the ground-state band in the mirror nucleus ^{55}Co supports the argument for the $11/2^-$ spin assignment [15,16].

The Coulomb excitation experiment on ^{55}Ni was performed at the Coupled Cyclotron Facility [17] of the National Superconducting Cyclotron Laboratory at Michigan State University. A primary beam of ^{58}Ni was accelerated in the K500 and K1200 cyclotrons to an energy of 140 MeV/nucleon. The primary beam was then incident on a 423 mg/cm² ^9Be fragmentation target to produce the secondary beam cocktail containing ^{55}Ni with an energy of 84.8 MeV/nucleon and an intensity of approximately 680 s⁻¹, purified in the A1900 fragment separator [18], and transported to the experimental area. The relatively low beam purity of 5% ^{55}Ni only, inherent to projectile fragmentation on the neutron-deficient side of the nuclear chart, was manageable due to event-by-event particle identification.

A 257.7 mg/cm² ^{197}Au Coulomb excitation target (77.2 MeV/nucleon midtarget energy) was placed in the center of SeGA, an array of eighteen, thirty-two-fold segmented, high-purity germanium detectors [19]. Identification of the ^{55}Ni particles of interest was performed on an event-by-event basis with the focal plane detectors of the S800 spectrograph [20,21] and two beam-monitoring plastic scintillators before the target. The SeGA array of germanium detectors was arranged in two rings, denoted as the 37° and 90° rings referring to the angle of the detectors with respect to the beam axis. For the present experiment, the SeGA array contained a total of 15 detectors, seven in the 37° ring and eight in the 90° ring.

*Present address: Lawrence Livermore National Laboratory, Livermore, CA 94550.

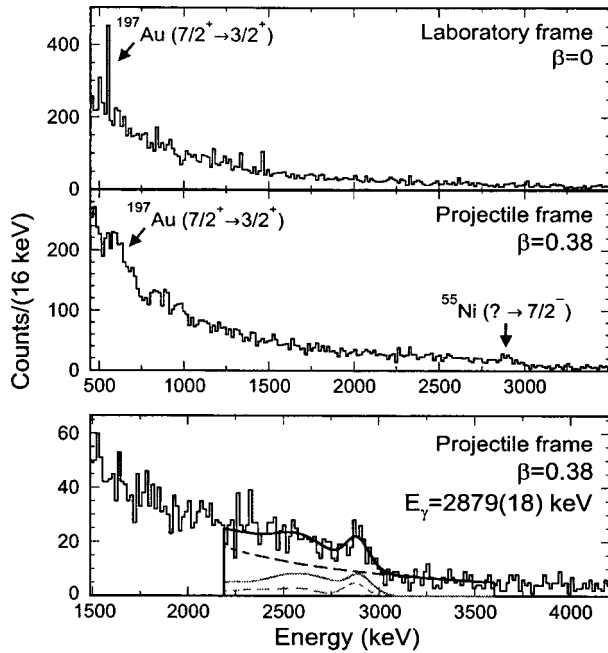


FIG. 1. Laboratory-frame (top) and projectile-frame (middle) γ -ray spectra in coincidence with ^{55}Ni particles. The γ rays from the deexcitation of an excited state of ^{55}Ni are apparent in the middle panel at about 2880 keV. Only the ^{197}Au deexcitation γ rays detected in the 90° ring of SeGA can be seen in the middle panel, as the γ rays are Doppler shifted to approximately 410 keV in the 37° ring. The bottom panel shows an expansion of the projectile-frame spectrum with fits overlaid. The solid black line is the total fit which contains the sum of the simulated response functions for the 37° (solid gray line) and 90° (dashed gray line) rings. The double-exponential background is indicated by the dot-dashed line.

GEANT [22] simulations were performed for the observed γ -ray energy to model the deexcitation spectrum of ^{55}Ni detected with SeGA. The Monte Carlo simulation was performed for ten million incident γ rays at a given energy, isotropically emitted in the projectile frame and Lorentz boosted with the mid-target beam velocity. The simulated histograms were fit with analytical curves to determine the area under the simulated photopeak, and thus the simulated efficiency. The analytical curves were then fit to the experimental spectrum. More details on the experimental setup and the data analysis have been previously discussed in [9,23,24].

The γ -ray spectra in coincidence with all ^{55}Ni particles satisfying the particle identification gates are shown in Fig. 1. A γ ray at approximately 2800 keV from the deexcitation of ^{55}Ni is visible in the projectile-frame spectrum. The simulated peak shapes for the two rings were simultaneously fit to the summed projectile-frame spectrum on top of a double-exponential background. The result of the fitting process is shown in the bottom panel of Fig. 1. γ -ray energies of 2882(11) and 2868(22) keV were measured for the 37° and 90° rings of SeGA, respectively. The weighted average of 2879(18) keV (including a 0.5% systematic uncertainty attributed to the Doppler reconstruction) agrees with the 2882 keV γ ray measured in the high-spin Gammasphere experiment [15].

The experimental cross section for Coulomb excitation is

$$\sigma = \frac{N_\gamma}{\epsilon_{tot} \times N_{beam} \times N_{target}}, \quad (1)$$

where N_γ is the number of detected deexcitation photons, ϵ_{tot} is the total detector efficiency, N_{beam} is the number of incident secondary beam nuclei, and N_{target} is the number of target nuclei per unit area. The total efficiency (ϵ_{tot}) includes contributions from the detector efficiency, solid angle covered by the detector array, angular distributions of emitted γ rays due to the reaction mechanism and Lorentz boost, and absorption of γ rays in the target material.

In heavy-ion scattering well above the Coulomb barrier, nuclear contributions to the electromagnetic excitation mechanism have to be excluded by restricting the analysis to events at extremely forward scattering angles. As the minimum impact parameter of the collision is related to the scattering angle [1,3], a maximum laboratory scattering angle of $\theta_{lab}^{max} = 3.1^\circ$ was chosen to assure the minimum impact parameter $b_{min} = 14.1$ fm to exceed the sum of target and projectile radius by 2.3 fm and consequently the interaction radius (following Wilcke *et al.* [25]) by 0.7 fm.

A gate on the appropriate scattering angle was not possible for ^{55}Ni due to low statistics and efficiency of the cathode-readout drift chambers used to reconstruct the laboratory scattering angle. Thus a method of scaling the measured cross section using the dependence of the ^{52}Fe cross section [9,24] on laboratory scattering angle was developed and tested and used to determine the Coulomb excitation cross section for ^{55}Ni in the present study. A detailed description of the method is presented in [9].

Assuming spin and parity of $11/2^-$ for the state—thus pure $E2$ character of the excitation—a total cross section of 89(19) mb was calculated using the number of γ rays determined from the fit in Fig. 1. With the scaling method and $S_\theta = 0.64$ for $\theta_{lab}^{max} = 3.1^\circ$ an integrated Coulomb excitation cross section of 57(16) mb was determined. The Alder-Winther theory of relativistic Coulomb excitation [1] was used to translate the measured cross section into an absolute $E2$ excitation strength of $B(E2; 7/2^- \rightarrow 11/2^-) = 251(69) e^2 \text{fm}^4$. If the 2879(18) keV γ ray measured in this experiment is the result of a $9/2^- \rightarrow 7/2^-$ transition, both $M1$ and $E2$ transitions are most probable.

The mixing of the two types of transitions can occur both in the excitation and deexcitation processes. The calculation of $B(\pi\lambda; 7/2^- \rightarrow 9/2^-)$ is dependent on the amount of each type of transition contributing to the excitation to the $9/2^-$ state. In the excitation process, the $E2$ multipolarity transition is expected to dominate. An upper limit of 4.9 mb excitation cross section for pure $M1$ was calculated using the recommended upper limits on $M1$ transition rates [26]. As the measured cross section using the scaling method was 57(16) mb, at least 92% of the excitation cross section is of type $E2$. The error on the measured $B(E2; 7/2^- \rightarrow 9/2^-)$ was adjusted to account for up to 8% contribution from $M1$ excitation. For the deexcitation process, the $M1$ transition is expected to dominate due to the transition rate favoring $M1$ deexcitation. The amount of each type of transition is impor-

TABLE I. Theoretical predictions for the excitation of the $11/2^-$ and $9/2^-$ members of the core-coupled multiplet in ^{55}Ni . Given are the results of a shell-model calculation employing the GXPF1 effective interaction using two different sets of effective charges: (A) $e_p = 1.5e, e_n = 0.5e$ and (B) $e_p = 1.3e, e_n = 0.7e$. In the last columns we give the value predicted by the core excitation model [6] outlined in the text, using the experimental $B(E2\uparrow)_{\text{core}} = 532(100) e^2 \text{fm}^4$ as well as the shell-model $B(E2\uparrow)_{\text{core}} = 702 e^2 \text{fm}^4$ excitation strength for ^{56}Ni . A_p and A_n are the proton and neutron strength amplitudes within the shell model.

Theory						
$B(E2; 7/2^- \rightarrow J_f)[e^2 \text{fm}^4]$						
$7/2^- \rightarrow J_f$	A_p	A_n	SM (A)	SM (B)	weak coupling (Expt.)	weak coupling (Theor.)
$J_f = 11/2^-$	19.38	13.23	159	148	160(30)	211
$J_f = 9/2^-$	18.39	21.42	183	189	133(25)	173
Experiment						
$B(E2; 7/2^- \rightarrow J_f)[e^2 \text{fm}^4]$						
$J_f^\pi = 11/2^-$	251(69)					
$J_f^\pi = 9/2^-$	$257_{+73}^{(-95)} e^2 \text{fm}^4$					

tant for the calculation of angular distribution effects modifying the γ -ray detection efficiency and thus entering the calculation of the total cross section. Using the recommended upper limits on $E2$ and $M1$ transition rates [26], a maximum contribution of 29% from $E2$ deexcitation transitions was calculated. Total cross sections calculated with mixings of 29%, 0%, and 100% $E2/M1$ fractions differed by less than 1%. An error of 1% was added to the calculated cross sections and transition probabilities for the $7/2^- \rightarrow 9/2^-$ transition to account for this uncertainty caused by the unknown $M1/E2$ mixing. The deduced excitation strength $B(E2; 7/2^- \rightarrow 9/2^-)$ equals $257_{+73}^{(-95)} e^2 \text{fm}^4$ derived from the cross section following [1].

A shell-model calculation of reduced transition probabilities to the observed excited state of ^{55}Ni was performed with the conventional shell-model code MSHELL [27] with the GXPF1 interaction [10,28]. The transition strengths were calculated as described in [29]. The calculation allowed for the excitation of seven particles out of the $f_{7/2}$ orbit. The calculations were performed with two different sets of total effective charges e_p and e_n . The results of the shell-model calculations are summarized in Table I with the $B(E2)$ values within the shell model deduced from the strength amplitudes and effective charges following

$$B(E2; 7/2^- \rightarrow J_f) = \frac{1}{8} (A_p e_p + A_n e_n)^2. \quad (2)$$

Figure 2 shows the low-lying $E2$ strength in ^{55}Ni calculated within the shell model (GXPF1 effective interaction, effective charges $e_p = 1.5e$ and $e_n = 0.5e$).

The core excitation model for the nondeformed, odd- A nuclei [6] based on the extreme case of weak coupling and ignoring a possible mixing of the $7/2^-$ ground state and the $7/2_2^-$ excited state, predicts with

$$B(E2; 7/2^- \rightarrow J^-) = \frac{2J+1}{8} \frac{B(E2\uparrow)_{\text{core}}}{5} \quad (3)$$

for $J \in \{3/2^-, 5/2^-, 7/2^-, 9/2^-, 11/2^-\}$, excitation strengths similar to the present shell-model calculation. Using the weighted mean $B(E2\uparrow) = 532(100) e^2 \text{fm}^4$ for the excitation of the first 2^+ state in the core ^{56}Ni [9], one expects $B(E2; 7/2^- \rightarrow 11/2^-) = 160 e^2 \text{fm}^4$ and $B(E2; 7/2^- \rightarrow 9/2^-) = 133 e^2 \text{fm}^4$. Table I lists the results for the weak coupling calculation using the experimental as well as the shell model $B(E2\uparrow)_{\text{core}}$ for ^{56}Ni .

Unlike the case of weak coupling where the summed $E2$ strength $\sum_{\text{multiplet}} B(E2\uparrow) = B(E2\uparrow)_{\text{core}}$ is expected to be concentrated at about $E(2_1^+) = 2.7 \text{ MeV}$ (^{56}Ni core), the shell model calculation for ^{55}Ni predicts 83.3% of the shell model $B(E2\uparrow)_{\text{core}} = 702 e^2 \text{fm}^4$ strength below 3.5 MeV and only 63.8% concentrated between 2.5 MeV and 3.0 MeV (see Fig. 2).

The measured reduced transition probability for either excited state spin and parity considered for the ^{55}Ni nucleus is

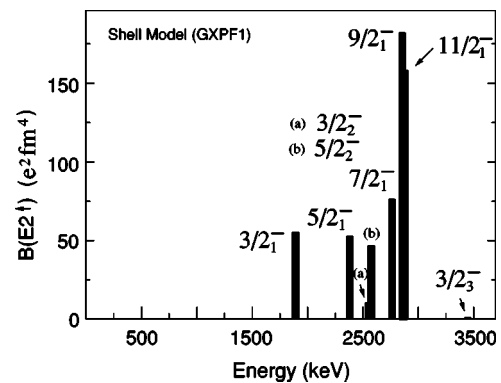


FIG. 2. Low-lying $E2$ strength in ^{55}Ni calculated within the shell model using the GXPF1 effective interaction and the effective charges $e_p = 1.5e$ and $e_n = 0.5e$.

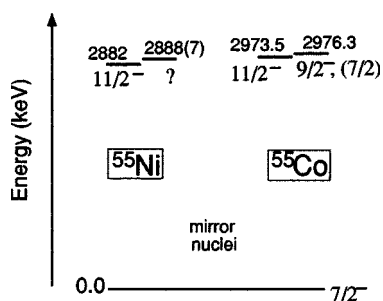


FIG. 3. Comparison of the ^{55}Ni level scheme with the mirror nucleus ^{55}Co [16]. We note that the first 2^+ state of ^{56}Ni lies at 2700.6(7) keV, supporting the assumption that the observed state(s) could correspond to a member or members of the core-coupled quintuplet of negative parity $2_1^+(^{56}\text{Ni}) \otimes \nu f_{7/2}^{-1}$.

higher than the values predicted within the shell model and the weak-coupling approach. One possible explanation for this discrepancy is that the measured peak at 2879(18) keV could be a doublet of γ rays very close in energy. The mirror nucleus ^{55}Co , with ground state spin and parity $7/2^-$, has an excited state with $J^\pi=11/2^-$ at 2973.48(20) keV and another with $J^\pi=9/2^-$ at 2976.34(19) keV [16] (Fig. 3). While a spin of $J=7/2$ has also been suggested for the higher-energy state, there is stronger evidence for $J^\pi=9/2^-$. If the γ ray measured at 2879(18) keV deexcites a doublet of states with energies less than 5 keV apart and spin and parity $9/2^-$ and $11/2^-$, it would appear as one γ ray within the present experimental conditions.

Then the measured $B(E2)$ value would have to roughly compare to the sum of the absolute excitation strengths to the $11/2^-$ and $9/2^-$ excited states predicted by theory.

In summary, absolute $B(E2)$ excitation strength in ^{55}Ni has been measured in intermediate-energy Coulomb excitation. The γ ray observed at 2879(18) keV is interpreted to correspond to the ground-state decay of the $11/2^-$ or $9/2^-$ member of the core-coupled quintuplet of negative parity $2_1^+(^{56}\text{Ni}) \otimes \nu f_{7/2}^{-1}$. The results exceed the values predicted within a large-scale shell-model calculation using the GXPF1 effective interaction and are higher than the values expected in an extremely simplified picture of weak coupling. In the mirror nucleus ^{55}Co , the candidates for the $11/2^-$ or $9/2^-$ states form a doublet that would hardly be resolved in an inverse-kinematics experiment with low statistics and a limit in resolution posed by the use of fast beams. This situation cannot be ruled out for the present study of ^{55}Ni .

We thank A. Stolz, T. Ginter, M. Steiner and the NSCL cyclotron operations group for providing the high-quality secondary and primary beams. We acknowledge fruitful discussions with A. F. Lisetskiy. This work was supported by the National Science Foundation under Grants No. PHY-0110253, PHY-9875122, PHY-0244453, INT-0089581 and in part by Grant-in-Aid for Specially Promoted Research (13002001) from the MEXT of Japan, and by the joint large-scale nuclear-structure calculation project by RIKEN and CNS.

- [1] A. Winther and K. Alder, Nucl. Phys. **A319**, 518 (1979).
 [2] T. Motobayashi *et al.*, Phys. Lett. B **346**, 9 (1995).
 [3] T. Glasmacher, Annu. Rev. Nucl. Part. Sci. **48**, 1 (1998).
 [4] H. Scheit *et al.*, Phys. Rev. Lett. **77**, 3967 (1996).
 [5] O. Sorlin *et al.*, Phys. Rev. Lett. **88**, 092501 (2002).
 [6] A. De Shalit, Phys. Rev. **122**, 1530 (1961).
 [7] G. Kraus *et al.*, Phys. Rev. Lett. **73**, 1773 (1994).
 [8] Y. Yanagisawa *et al.*, in *ENAM 98, Exotic Nuclei and Atomic Masses*, edited by Bradley M. Sherrill, David J. Morrissey, and Cary N. Davids, AIP Conf. Proc. No. 455 (AIP, New York, 1998), p. 610.
 [9] K. L. Yurkewicz *et al.*, Phys. Rev. C **70**, 054319 (2004).
 [10] M. Honma, T. Otsuka, B. A. Brown, and T. Mizusaki, Phys. Rev. C **69**, 034335 (2004).
 [11] J. A. Cameron and B. Singh, Nucl. Data Sheets **102**, 293 (2004).
 [12] P. Hornshoj, L. Hojsolt-Poulsen, and N. Rud, Nucl. Phys. **A288**, 429 (1977).
 [13] J. Äystö *et al.*, Phys. Lett. **138B**, 369 (1984).
 [14] D. Mueller, E. Kashy, and W. Benenson, Phys. Rev. C **15**, 1282 (1977).
 [15] D. Rudolph *et al.*, Z. Phys. A **358**, 379 (1997).
 [16] H. Junde, Nucl. Data Sheets **64**, 723 (1991), updated 2001.
 [17] F. Marti, D. Poe, M. Steiner, J. Stetson, and X. Y. Wu, in *Proceedings of the 16th International Conference on Cyclotrons and Their Applications*, edited by Felix Marti, AIP Conf. Proc. No. 600 (AIP, New York, 2001), p. 64.
 [18] D. J. Morrissey, B. M. Sherrill, M. Steiner, A. Stolz, and I. Wiedenhoever, Nucl. Instrum. Methods Phys. Res. B **204**, 90 (2003).
 [19] W. F. Mueller, T. Glasmacher, D. Gutknecht, G. Hackman, P. G. Hansen, Z. Hu, K. L. Miller, and P. Quirin, Nucl. Instrum. Methods Phys. Res. A **466**, 492 (2001); W. F. Mueller *et al.*, Nucl. Phys. **A734**, 418 (2004).
 [20] D. Bazin, J. A. Caggiano, B. M. Sherrill, J. Yurkon, and A. Zeller, Nucl. Instrum. Methods Phys. Res. B **204**, 629 (2003).
 [21] J. Yurkon, D. Bazin, W. Benenson, D. J. Morrissey, B. M. Sherrill, D. Swan, and R. Swanson, Nucl. Instrum. Methods Phys. Res. A **422**, 291 (1999).
 [22] GEANT, Technical Report W5013, CERN, 1994.
 [23] A. Gade *et al.*, Phys. Rev. C **68**, 014302 (2003).
 [24] K. L. Yurkewicz *et al.*, Phys. Rev. C **70**, 034301 (2004).
 [25] W. W. Wilcke, J. R. Birkelund, H. J. Wollersheim, A. D. Hoover, J. R. Huizenga, W. U. Schröder, and L. E. Tubbs, At. Data Nucl. Data Tables **25**, 391 (1980).
 [26] P. M. Endt, At. Data Nucl. Data Tables **23**, 547 (1979).
 [27] T. Mizusaki, RIKEN Accel. Prog. Rep. **33**, 14 (2000).
 [28] M. Honma, T. Otsuka, B. A. Brown, and T. Mizusaki, Phys. Rev. C **65**, 061301 (2002).
 [29] B. A. Brown and B. H. Wildenthal, Phys. Rev. C **21**, 2107 (1980).